7A.1   Impact of Fall Speed Computations on the Structure of Mesoscale Convective Systems in
Spectral and Bulk Microphysical Schemes

Eric A. Aligo[*] and W. A. Gallus, Jr.
Iowa State University, Ames, Iowa

1. INTRODUCTION

Since Mesoscale Convective Systems (MCSs) represent the major source of warm-season rainfall for the central and northern Plains (Fritsch et al. 1986), it is important to have high quality rainfall forecasts of such systems. Additionally, different types of MCS morphologies (linear systems including leading and trailing stratiform) produce various forms of hazardous weather (Doswell 1996), thus forecasting the correct morphology is also important. Gallus et al. (2008) showed that trailing stratiform (TS) systems were most often associated with wind damage, while leading stratiform (LS) systems were most often associated with hail and tornadoes. Parker and Johnson (2000) showed that the placement of the stratiform rain in linear MCSs is determined by how hydrometeors are advected away from the main updraft region by the mean mid-upper level wind flow relative to the storm. The TS systems were associated with front-to-rear storm-relative winds, while LS systems with weak middle and upper-tropospheric rear-to-front storm relative winds.

Many studies have performed sensitivity tests evaluating the impact of varying uncertain parameters in microphysical schemes on precipitation by varying the slope intercept, particle density (Gilmore et al. 2004b) as well as constants in fall speed equations (Colle and Mass 2000) and the definition of particle size (Potter 1991). Some studies have pointed out the importance of ice (Potter 1991) as well as θ_e and precipitation fallout (Gallus and Johnson 1995) in the development of the stratiform region of convective systems.

The LS systems, although initially forming in a favorable wind shear environment, are believed to be sustained by microphysical processes (Parker, 2004b). Melting and evaporation of precipitation in the stratiform region of LS systems destabilizes the atmosphere, while pressure patterns induced by these processes lead to ascent on inflowing air parcels in and ahead of the leading precipitation.

Lynn and Khain (2007) performed 3-D runs of a squall line associated with a sea-breeze event and showed a reduction in surface rain rates and a more well defined stratiform cloud structure that were both closer to observations in their spectral (bin) microphysical scheme as compared to bulk microphysical schemes. They believe the bulk scheme approach for computing fall speeds forces smaller particles to fall out together with the larger particles instead of being advected into and contributing to the stratiform region of the squall line.

The authors of this study make an attempt to determine if the bulk microphysical scheme assumptions for terminal fall speed produces incorrectly intense precipitation in a more confined area over a short period of time and does not replicate properly the structure of stratiform clouds, inaccuracies that possibly be avoided by using bin schemes. Additional tests will determine if LS and TS systems both have different sensitivities to the modifications of the fall speeds because of the differences in kinematic profiles as well as the microphysical processes between the two types of systems.

The experiments in this paper will include the use of a bin scheme, and a bulk scheme with various modifications to the fall speeds of all particles in both the bin and bulk schemes. A description of the experiments follow.

2. DATA AND METHODOLOGY

Two dimensional (2-D) idealized Weather Research and Forecast (WRF) Advanced Research WRF (ARW) model (Skamarock et al. 2005) runs were performed using a bin microphysical scheme that, as a result of computational requirements, can not be run in three dimensions (3-D). The version that will be used in this study is described in Geresdi (1998) and Rasmussen et al. (2002) (hereafter denoted as the Geresdi scheme) and was obtained through Greg Thompson.

The idealized runs in this study simulate a squall line in the x direction (east-west) and will be initialized with wind data from Parker and Johnson (2000) that represents a composite of TS and LS systems. The sounding used to

Corresponding author address: Eric A. Aligo,
ISU, Agronomy Hall 3010, Ames, IA. Email:
ealigo@iastate.edu

initialize the 2-D runs is shown in Fig. 1 with a wind profile representative of a TS system, and temperature and moisture data from a modified version of the Weisman et al. (1988) sounding. The modification included an increase in moisture throughout the depth of the atmosphere to increase the extent of the stratiform region produced by the system.
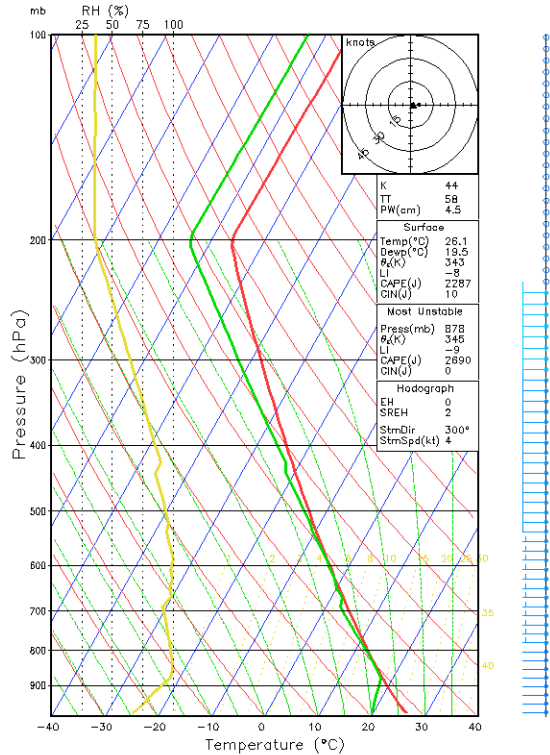
Figure. 1:   Skew T-log*p* diagram of sounding used in 2-D simulations with TS wind profile.

Convection is initiated with a warm thermal perturbation, and the simulations were integrated out to seven hours using a horizontal grid spacing of 1 km, 31 vertical levels and 600 points in the x-direction. The idealized runs use a simplified orography, do not consider radiation, surface fluxes or frictional effects. The boundary conditions are open in the x-direction and periodic in the y-direction.

WRF 3-D real runs were performed using a 1 km domain nested within a 4 km and 12 km domain with the simulated cases located in the Midwest. The model physical configuration for the 3-D runs is that described in Aligo et al. (2007) with the exception of the planetary boundary layer (PBL) scheme and the land surface model (LSM), which in the present study are, respectively, the Mellor-Yamada-Janjic (MYJ; Janjic 2002) scheme and the Noah LSM (Ek et al. 2003). In addition to the above

configuration, the 12 km outer domain used the Betts-Miller-Janjic convective scheme (Betts 1986; Betts and Miller 1986; Janjic 1994), which currently is used operationally at NCEP.

The NARR, which is used in the present study for the 3-D runs only, contains data on 29 pressure levels, has a vertical grid spacing of 25 hPa below 700 hPa and above 300 hPa and a vertical grid spacing of 50 hPa between these two levels.

The 3-D real evaluations focused on the 30-31 May 2003 (Fig. 2) and 09-10 June 2003 cases (Fig. 3) using the NARR for the IC and LBC. The case in Fig.2 represents a TS system, while the case in Fig. 3 represents an LS system from the Bow Echo and Mesoscale Convective Vortex Experiment (BAMEX; Davis et al. 2004).
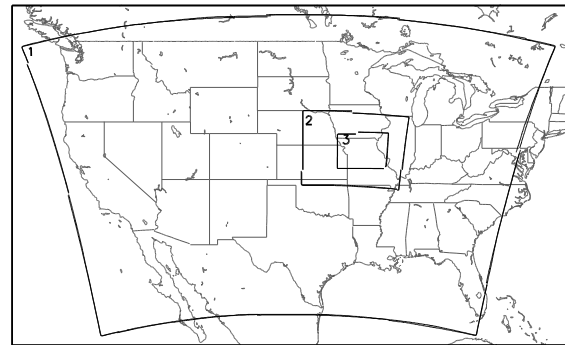
Figure 2: Locations of the 12 km, 4 km and 1 km simulation domains for the 30-31 May 2003 case.
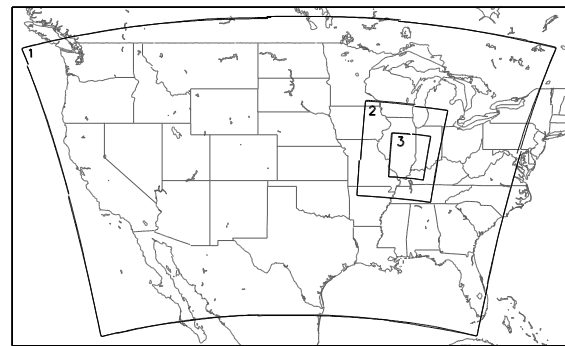
Figure 3: Same as Fig. 2 but for the 09-10 June 2003 case.

3. PLAN DESCRIPTION

WRF 2-D idealized simulations of TS and LS systems were performed using the Geresdi bin scheme, the Thompson bulk scheme (Thompson et al. 2006), a version of

the Geresdi scheme using fall speed relations typically found in a bulk scheme (hereafter termed Geresdi_I), and a version of the Thompson scheme using fall speed values from the bin scheme (hereafter termed Thompson_I).

The Geresidi_I scheme is identical to the Geresdi scheme with the exception of how the values of the ice,snow,liquid and graupel fall speeds are treated for each of the 36 mass-doubling bins. Instead of diameter-dependent fall speeds for each bin as is the case in the Geresdi scheme and in all bin schemes, the Geresdi_I run has one fall speed assigned to each bin based on the mass-weighted terminal fall speed that is computed in bulk schemes ,including the Thompson scheme, and is given by:

$$\hat{V} \equiv \frac{\int_0^\infty V(D)m(D)N(D)dD}{\int_0^\infty m(D)N(D)dD}. \quad (1)$$

In the Thompson scheme, all falling particles follow the power law relation from Ferrier (1994):

$$V(D) = \left(\frac{\rho_0}{\rho}\right)^{1/2} \alpha D^\beta e^{-fD}, \quad (2)$$

where ρ_0 is ~ 1.18 kg m^{-3} and is the air density at 1013 hPa, ρ is the air density at a particular altitude, D is the diameter of the particle and α, β and f are constants with values of 40, 1 and 125, respectively, for snow. For ice, α, β and f are given the values 2247, 1 and 0, respectively. For rain and graupel, α, β and f are 4854, 1 and 195 and 130, 0.7 and 0, respectively. See Thompson et al. (2006) for a definition of $m(D)$ and $N(D)$.

In the Thompson_I run, the ice, snow, rain and graupel fall speeds from the Thompson run were replaced by those from the Geresdi scheme run at every time step using a sorting and probability matching technique (Ebert 2001).

In the Gersedi scheme, the fall speed for hexagonal plate ice crystals is:

$$V_i = 304D_i\left(\frac{1.2}{\rho_a}\right)^{0.5}, \quad i=1,\dots k, \quad (3)$$

and for rimed crystals,

$$V_i = 1250D(1.2/\rho_a)^{0.5} \quad (4)$$

if $m < 5.654$ x 10^{-9} kg,

$$V_i = 4.84D^{0.25}(1.2/\rho_a)^{0.5} \quad (5)$$

if $m \geq 5.654$ x 10^{-9} kg

,where D_i is the diameter of the particle for bin i, ρ_a is the density of air and k is the number of bins. For liquid particles, the velocities are based on the Best and Bon number approach as described in Pruppacher and Klett (1997). Graupel particle velocities are specified in Rasmussen and Heymsfield (1987).

The computational expenses associated with a bin scheme prevent one from running the Geresdi scheme in 3-D. However, to extend the work into 3-D, the Thompson_I experiment will be run in 3-D for the two real cases described above.

4. PRELIMINARY RESULTS

4.1 *Bin versus Bulk*

Hovmoller diagrams of rain rate (in. h^{-1} ; 1 in. = 25.4 mm) from the Thompson and Geresdi scheme runs over a seven hour period are shown in Figs. 4 and 5, respectively. Clearly, the Thompson scheme develops a stratiform region earlier and maintains a much wider stratiform region than in the bin scheme, contrary to expectations.
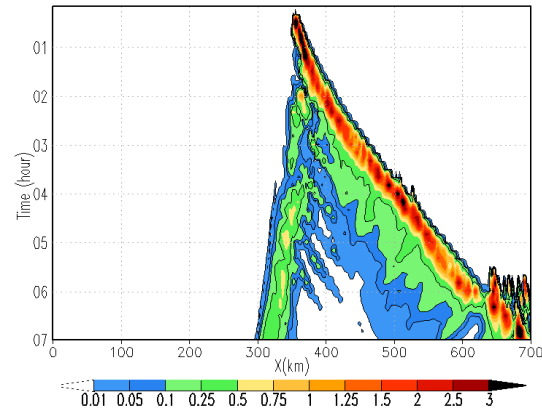
Figure 4: Hovmoller diagram of rain rate (in. h^{-1} ; 1 in. = 25.4 mm) for the run using the Thompson scheme over the seven hour integration period.
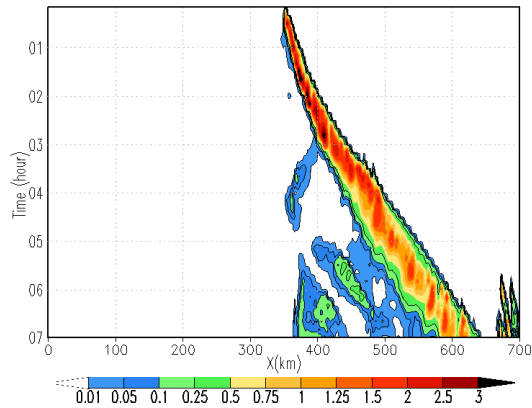
Figure 5: Same as in Fig. 4 but for the Geresdi scheme.

A vertical cross section of radar reflectivity for the TS system shortly after five hours into the simulation also reveals a much wider stratiform region in the Thompson scheme (Fig. 6a,b). However, the convective rain rates are somewhat weaker in the Geresdi scheme, a result that was anticiptated.
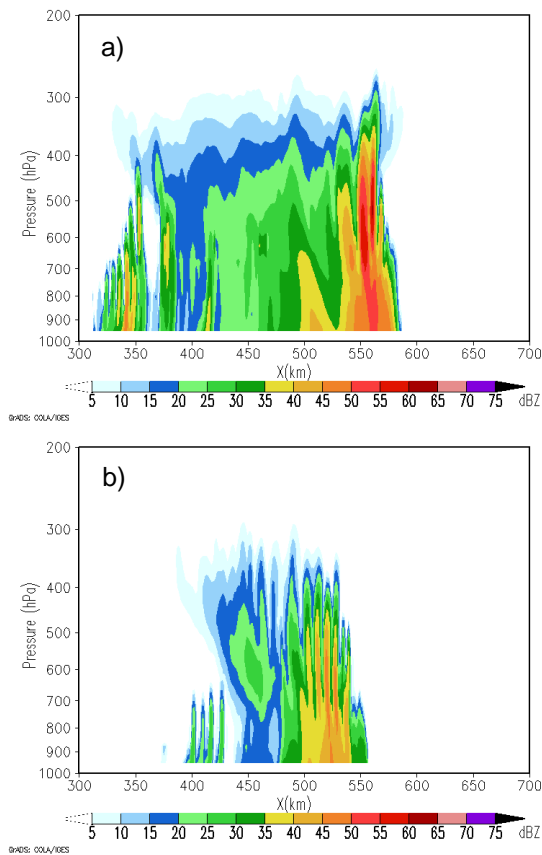
Figure 6: Vertical cross sections of simulated radar reflectivity shortly after 5 hours into the simulation for the (a) Thompson and (b) Geresdi

schemes. Units of reflectivity are dBZ.

4.2 *Fall speed modifications*

When mass-weighted terminal fall speeds were computed in Geresdi_I, there was only a minor affect on the stratiform region of the system (Fig. 5 and Fig. 7). The largest impact of the fall speed modifications occurred in the convective region with more intense rainfall occurring in Geresdi_I, as was expected. Frequent rain rates of at least 3 in. h^{-1} (76.2 mm h^{-1}) were simulated in Geresdi_I, amounts rarely simulated in the Geresdi run. Note no model data were available for hours six and seven in Geresdi_I.
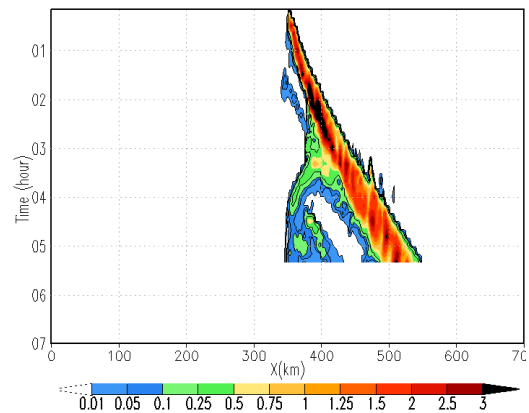
Figure 7: Hovmoller diagram of rain rate (in. h^{-1}) for Geresdi_I for approximately 5 hours of integration time. Note no model data were available for hours six and seven.

For experiment Thompson_I, fall speeds were extracted from the mature stage of the bin run, and were fed into the Thompson scheme. Figure 8 is a Hovmoller diagram of rain rate (in. h^{-1}) from Thompson_I and shows the rain rates in the stratiform region to be slightly better defined and the stratiform region to be slightly more extensive (Fig. 4 and Fig. 8). Rain rates in the convective region were also slightly weaker, as anticipated.
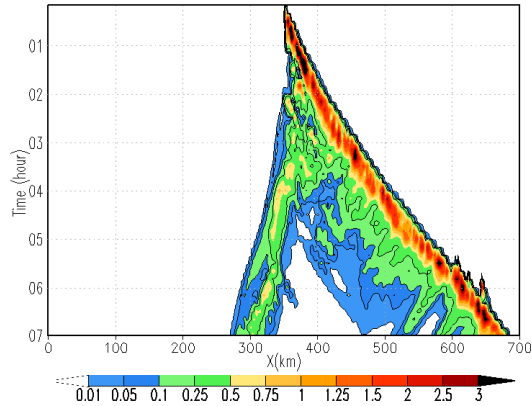
Figure 8: Hovmoller diagram of rain rate (in h^{-1}) for Thompson_I for seven hours of integration.

A time series of accumulated rainfall for 6 selected grid points shows the Geresdi scheme often with more accumulated rainfall than the Thompson scheme (Fig. 9) likely due to the Geresdi schemes slower moving system and wider convective region. Note the location of the grid points are indicated on the top left portion of each panel in Fig. 9, and can be easily identified in Fig. 8. The TS system progressed faster in the Thompson scheme than in the Geresdi scheme by 15 minutes early on to as much as 30 minutes when the system was mature. Also, Geresdi_I has a stronger convective rain rate, as expected, indicating that perhaps the use of the mass-weighted terminal fall speeds in the bin scheme resulted in more smaller particles falling out with the larger particles in the convective region. Additionally, the stratiform rain rates in Thompson_I appear stronger than in Thompson, while the convective rain rates generally appear weaker. This is consistent with the idea that the bin scheme better captures the fall speed distributions and incorporating bin fall speeds into the bulk scheme results in more smaller particles being advected away from the main updraft region and contributing to the stratiform region, while also leading to smaller convective rain rates.
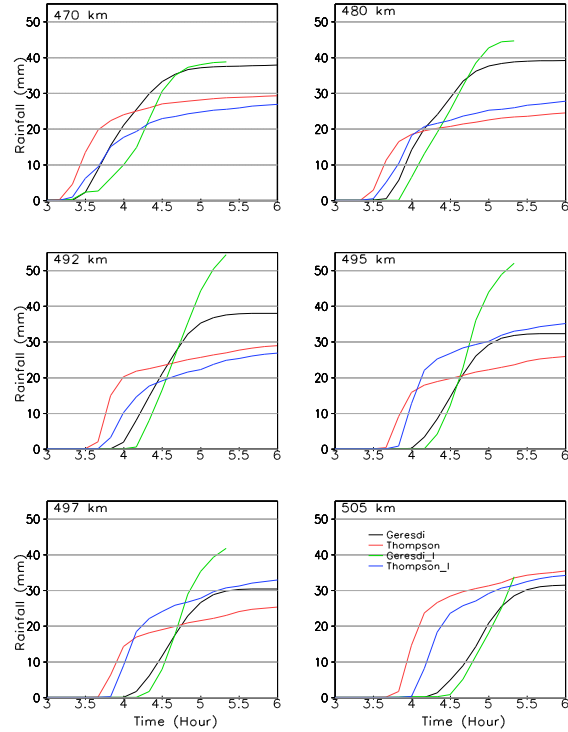
Figure 9: Time series of accumulated rainfall (mm) for six points from various experiments indicated within the plot above. The location of the grid points are indicated on the top left portion of each panel in the above figure and can be easily identified in Fig. 8.

An analysis of fall speeds from Thompson and Thompson_I averaged over the entire domain (Fig. 10) shows Thompson_I snow fall speeds lower for most of the integration period and with graupel fall speeds lower during the first two hours of the simulation. This could help explain the slightly larger stratiform rain rate, as shown earlier in Thompson_I as slower falling particles were suspended longer and able to be advected away from the main updraft region. The effects of the larger Thompson_I rain fall speeds were likely limited as rain particles would not be expected to play a major role in developing the stratiform region due to their relatively short duration within the troposphere.
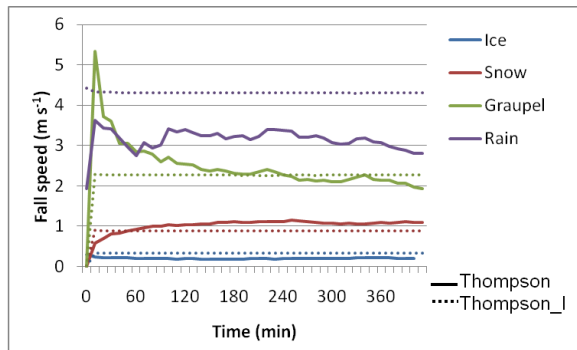
Figure 10: Time series of domain-averaged fall speeds of ice,snow,graupel and rain for Thompson and the Thompson_I.

5. SUMMARY

The Geresdi 2-D simulation of a TS system had a weaker stratiform region than that simulated by the Thompson scheme, a result not anticipated. However, implementing the mass-weighted terminal fall speed relations from the Thompson scheme into the bin scheme resulted in the bin scheme having larger convective rain rates, a result that was expected. Additionally, using the fall speed distributions from the bin scheme run to drive the Thompson scheme run resulted in a convective rain rate that was slightly lower and a stratiform rain rate that was larger compared to the control Thompson simulation. Additionally, the spatial extent of the stratiform region was slightly larger in the Thompson_I run, the run driven by bin fall speeds. It was determined that Thompson_I generally had lower fall speeds for snow and ice suggesting that these particles might have been suspended for a longer period of time and advected farther away from the main updraft region reducing the convective rain and creating a larger stratiform region.

6. FUTURE WORK

Additional work includes using an improved method for incorporating the Geresdi scheme fall speeds into the Thompson scheme. Instead of using bin fall speeds from a specified time interval (the mature stage as was done here), it might be more appropriate to separate the fall speeds into those associated with convective rainfall and those with stratiform rainfall. The purpose for this change is the recognition that fall speed distributions could vary between the convective and stratiform regions and likely during the early and mature stages of the system.

This work focused on a TS case and an extension to an LS case is underway. Additionally, a careful evaluation of the microphysical and dynamic processes involved in the experiments will be examined in the 2-D cases as well as 3-D cases and with different soundings. Additional testing with a higher vertical grid resolution is also underway.

7. ACKNOWLEDGEMENTS

8. REFERENCES

Aligo, E.A., W.A. Gallus, Jr., and M. Segal, 2007: Summer rainfall forecast spread in an ensemble initialized with different soil moisture analyses. *Wea. Forecasting*, **22,** 299-314.

Betts, A.K., 1986: A new convective adjustment scheme. Part I: Observational and theoretical basis. *Quart. J. Roy. Meteor. Soc.*, **112,** 677-692.

____, and M.J. Miller, 1986: A new convective adjustment scheme. Part II: Single column tests using GATE wave, BOMEX, ATEX and arctic air-mass data sets. *Quart. J. Roy. Meteor. Soc.*, **112,** 693-709.

Colle, B. A., and C. F. Mass, 2000: The 5-9 February 1996 flooding event over the Pacific Northwest: Sensitivity studies and evaluation of the MM5 precipitation forecasts. *Mon. Wea. Rev.*, **128,** 593-617.

Davis, C., and Coauthors, 2004: The bow echo and MCV experiment: observations and opportunities. *Bull. Amer. Meteor. Soc.*, **85,** 1075-1093.

Doswell, C. A., III, H. E. Brooks, and R. A. Maddox, 1996: Flash flood forecasting: An ingredients-based methodology. *Wea. Forecasting*, **11**, 560-581.

Ebert, E. E., 2001: Ability of a poor man's ensemble to predict the probability and distribution of precipitation. *Mon. Wea. Rev.*, **129**, 2461-2480.

Ek, M. B., K.E. Mitchell, Y. Lin, E. Rogers, P. Grunmann, V. Koren, G. Gayno, and J.D. Tarplay, 2003: Implementation of Noah land surface model advances in the National Centers for Environmental Prediction operational mesoscale Eta model. *J. Geophys. Res.*, **108,** 8851,

doi:10.1029/2002JD003296.

Ferrier, B. S, 1994: A double-moment multiple-phase four-class bulk ice scheme. Part I: Description. *J. Atmos. Sci.*, **51,** 249-280.

Fritsch, J. M., R. J. Kane, and C. R. Chelius, 1986: The contribution of mesoscale convective weather systems to the warm-season precipitation in the United States. *J. Climate Appl. Meteor.*, **25**, 1333-1345.

Gallus, W. A. Jr. and R. H. Johnson, 1995: The dynamics of circulations within the trailing stratiform regions of squall lines. Part I. The 10-11 June PRE-STORM system. *J. Atmos. Sci.*, **52,** 2161-2187.

_____, N. A. Snook and E. V. Johnson, 2008: Spring and summer severe weather reports over the Midwest as a function of convective mode: A preliminary study. *Wea. Forecasting.*, **23,** 101-113.

Geresdi, I, 1998: Idealized simulation of the Colorado hailstorm case: comparison of bulk and detailed microphysics. *Atmospheric Research,* **45**, 237-252.

Gilmore, M. S., J. M. Straka and E. N. Rasmussen, 2004b: Precipitation uncertainty due to variations in precipitation

Janjic, Z.I., 1994: The step-mountain Eta coordinate model: Further developments of the convection closure schemes. *Mon. Wea. Rev.*, **122,** 927-945.

_____, 2002: Nonsingular implantation of the Mellor-Yamada level 2.5 scheme in the NCEP meso model. NOAA/NWS/NCEP Office Note #437, 61 pp.

Lynn, B. and A. Khain, 2007: Utilization of spectral bin microphysics and bulk parameterization schemes to simulate the cloud structure and precipitation in a mesoscale rain event. *J. Geophys. Res.,* **112,** 22205, doi:10.1029/2007JD008475.

McCumber, M., W-K. Tao, J. Simpson, R. Penc ands-T Soong, 1991: Comparison of ice-phase microphysical parameterization schemes using numerical simulations of tropical convection. *J. Appl. Meteor.,* **30,** 985-1004.

Parker, D. M. and R. H. Johnson, 2000: Organizational modes of midlatitude mesoscale convective systems. *Mon Wea. Rev.*, **128,** 3413-3436.

_____, and _____, 2004b: Simulated convective lines with leading precipitation. Part II: evolution and maintenance. *J. Atmos. Sci.*, **61,** 1656-1673.

Potter, B. E., 1991: Improvements to a commonly used cloud microphysical bulk parameterization. *J. Appl. Meteor.,* **30,** 1040-1042.

Pruppacher, H. R., and J. D. Klett, 1997: *Microphysics of clouds and precipitation.* Kluwer Academic Publishers, 945 pp.

Rasmussen, R. M., and. A. J. Heymsfield, 1987: Melting and shedding of hail and graupel. Part I. Model physics. *J. Atmos. Sci*, **44**, 2754-2763.

_____, I. Geresdi, G. Thompson, K, Manning and E. Karplus, 2002: Freezing drizzle formation in stably stratified layer clouds: The role of radiative cooling of cloud droplets, cloud condensation nuclei, and ice initiation. *J. Atmos. Sci.*, **59,** 837-860.

Skamarock, W.C., J.B. Klemp, J. Dudhia, D.O. Gill, D.M. Barker, W. Wang, and J.G. Powers, 2005: A description of the advanced research WRF version 2. NCAR Tech. Note NCAR/TN-468+STR, 88 pp. [Available online at http://www.wrf-model.org/wrfadmin/docs/arw_v2.pdf]

Thompson, G., P. R. Field, W. D. Hall and R. M. Rasmussen, 2006: A new bulk microphysical parameterization for WRF (&MM5). Preprints, *7th WRF Users' Workshop,* Boulder, CO, National Center for Atmospheric Research, 1-11.

Weisman, M. L., J. B. Klemp, and R. Rutunno, 1988: Structure and evolution of numerically simulated squall lines. *J. Atmos, Sci.,* **45**, 1990-2013.